ARTICLE

# Control of Carrier Type and Density in Exfoliated Graphene by Interface Engineering

Rui Wang,[†,‡] Shengnan Wang,[†,§] Dongdong Zhang,[†,‡] Zhongjun Li,[†] Ying Fang,[†] and Xiaohui Qiu[†,*]

[†]National Center for Nanoscience and Technology, Zhongguancun, Beijing 100190, China, [‡]Academy of Advanced Interdisciplinary Studies, Peking University, Beijing, 100871, China, and [§]Department of Physics, Tsinghua University, Beijing, 100084, China

**ABSTRACT** Air-stable, n-doped or p-doped graphene sheets on a chip were achieved by modifying the substrates with self-assembled layers of silane and polymer. The interfacial effects on the electronic properties of graphene were investigated using micro-Raman and Kelvin probe force microscopy (KPFM). Raman studies demonstrated that the phonon vibrations were sensitive to the doping level of graphene on the various substrates. Complementary information on the charge transfer between the graphene and substrate was extracted by measuring the surface potential of graphene flakes using KPFM, which illustrated the distribution of carriers in different graphene layers as well as the formation of dipoles at the interface. The Fermi level of single layer graphene on the modified substrates could be tuned in a range from −130 to 90 mV with respect to the Dirac point, corresponding to the doped carrier concentrations up to $10^{12}$ $cm^{-2}$.

**KEYWORDS:** graphene · interface · doping · Raman · Fermi level

Graphene has attracted tremendous interest due to its unique electronic structure, ultrahigh mobility, and near ballistic transport characteristics.[1−3] Although the Fermi level of intrinsic graphene is expected to be at the Dirac point, recent electrical transport measurements often showed that most of the graphene transistors on $SiO_2$ substrates in air were p-doped.[4,5] When constructing combinatorial logic circuits, control of the carrier density in graphene, to realize both n- and p-type conductive channels, is desired. In silicon-based field effect transistors (FETs), ion implantation is a reliable method of carrier doping in the active channel.[6,7] However, the technique is not applicable to graphene because it will destroy the two-dimensional carbon structure. Alternative approaches that have been proposed include chemical doping by the adsorption of molecules[8] and the metal contacts,[9] which could efficiently alter the doping level due to the linear energy band structure of graphene.[1,2] The carrier concentration of graphene could also be tuned *via* the electrical field applied by back gate.[10]

Self-assembled layers on silicon substrates, such as silane and polymer, have been successfully used to enhance the mobility of organic thin film transistors[11] and to eliminate the Schottky barriers at the metal-semiconductor interfaces.[12,13] We adopted a similar approach to modify the interface between graphene flakes and the substrate in order to tune the carrier type and density of graphene on the chip. The effects of the interface on the doping level of graphene were investigated by micro-Raman and Kelvin probe force microscopy (KPFM). Raman characteristics of single layer graphene (SLG) on various substrates revealed the correlation of phonon vibrations with the carrier concentration. The formation of dipoles at the interface was further elucidated by KPFM, which enabled a quantitative measurement of charge transfer between the substrate and graphene.

## RESULTS AND DISCUSSION

Figure 1a shows the overall scheme of the experiment. Isolated graphene flakes on the substrates were achieved using mechanical exfoliation of natural graphite under ambient conditions.[1] Four types of substrates were used in the experiment, including silicon wafers coated with 270 nm thick polymethyl methacrylate (PMMA), silicon wafers capped with 300 nm silicon oxide ($SiO_2$), or $SiO_2$ surface modified with two kinds of silanes, $(CF_3)(CF_2)_5(CH_2)_2Si(OC_2H_5)_3$ and $(NH_2)(CH_2)_3Si(OC_2H_5)_3$, referred to as FTS and ATS, respectively. The silane modified $SiO_2$ surfaces were achieved by exposing the cleaned substrates to FTS and ATS vapors at room temperature for 6 h. The formation of silane layers on the substrate surfaces was confirmed by contact angle measurements (see Supporting Information, Table S1). An atomic force microscope (AFM) (Veeco Dimension 3100) with a conductive tip was used to per-

*Address correspondence to xhqiu@nanoctr.cn.

Received for review August 31, 2010 and accepted November 30, 2010.

**Published online December 6, 2010.** 10.1021/nn102236x

form the topographic and surface potential (SP) measurements under a dual-pass tapping mode. We used the Pt/Ir coated highly doped silicon tips (Veeco, SCM-PIT) with a nominal curvature radius of 15 nm. The tip lifted height was 10 nm. Therefore, the spatial resolution of the obtained surface potential images was estimated to be 30 nm.

Micro-Raman spectroscopy was employed to determine the layer number of the graphene films. SLGs are identified by the symmetric 2D band (~2680 $cm^{-1}$) and the relative intensities of the doubly degenerated G band (1580 $cm^{-1}$).[14,15] The Raman spectra of SLGs on various substrates are shown in Figure 1b. The absence of the defect-related D band indicated the high quality of the graphene samples.[15] The positions, intensities, and line widths of the G and 2D band varied significantly on different substrates, suggesting a pronounced influence of modified substrates on the electronic properties of graphene. Figure 2a plots the statistical analysis of the intensity ratio of the 2D band over the G band ($I$(2D)/$I$(G)) as a function of the G band position. The position of G band of SLGs shifted from 1575 $cm^{-1}$ on PMMA to 1595 $cm^{-1}$ on ATS. Additionally, $I$(2D)/$I$(G) decreased from 7 to 1 as the G band frequency increased. It was reported that the position of the G band shifted proportionally to both the electron and hole concentration of graphene under electric field modulation.[16,17] A decrease of $I$(2D)/$I$(G) was also observed as the G band shifted upward.[17] Our observations agree with these results and indicate that the doping level of SLG sheets could be tuned on the modified substrates. It should be noted that the intensity ratio $I$(2D)/$I$(G) of the SLG on the PMMA surface was much higher than those on the other substrates, implying that the SLG samples on the PMMA surface were close to the neutral state.

The stiffening of G band was accompanied with a decrease in the line-width of the G peak, as shown in Figure 2b. Earlier reports have demonstrated that the full width at half-maximum of the G band (fwhm (G)) was also sensitive to the carrier concentration of graphene, suggesting that the fwhm (G) is a direct measure of the doping level of graphene.[16,17] The fitted line, according to the nonadiabatic approximation in ref 18, described well the dependence of the fwhm as a function of the G band position. In ref 18, the stiffening and narrowing of the G band were interpreted in terms of the phonon−electron coupling in graphene as the Fermi level of the graphene sheets was tuned in an electric field. In our experiment, the similar characteristics in the Raman spectra indicated that the interface modification was also efficient in intentionally tailoring the electronic band structure of graphene.

The carrier type and density in the graphene sheets on different substrates were quantitatively studied using KPFM, which has been widely used to investigate the charge exchange between nanoparticles and substrates,[19,20] molecular doping on carbon nanotubes,[21] and the electrical complexity at the interface between pentacene films and a $SiO_2$ substrate.[22,23] Figure 3a−d shows the topography of several graphene sheets on $SiO_2$, FTS, PMMA, and ATS surfaces, respectively. The corresponding surface potential (SP) images of the samples are presented in Figure 3e−h. The SP

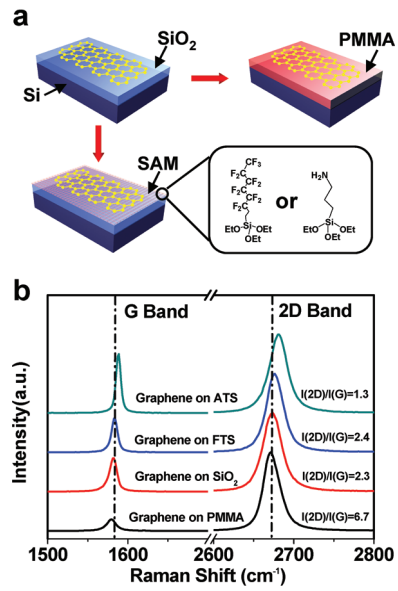


**Figure 1. (a) Schematic illustration of the chemical modification of substrates used in the experiment. (b) Typical Raman spectra of single layer graphene (SLG) on PMMA(black), $SiO_2$(red), FTS(blue), and ATS(green), respectively.**

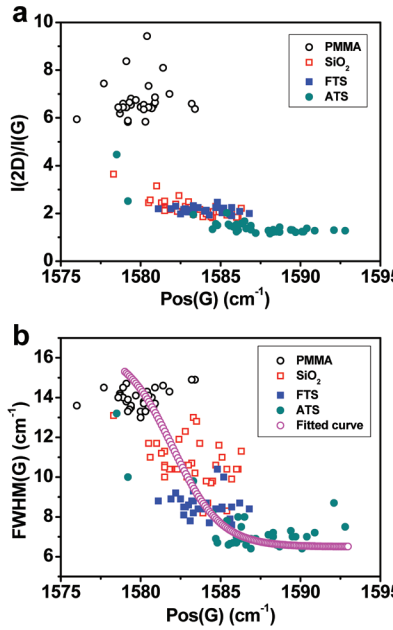


**Figure 2. Statistical analysis of Raman characteristics of the SLGs on various substrates: (a) ratio of intensity of the 2D band over the G band; (b) fwhm of the G band as a function of the position. The pink circle line in panel b is the predicted nonadiabatic trend from ref 18.**

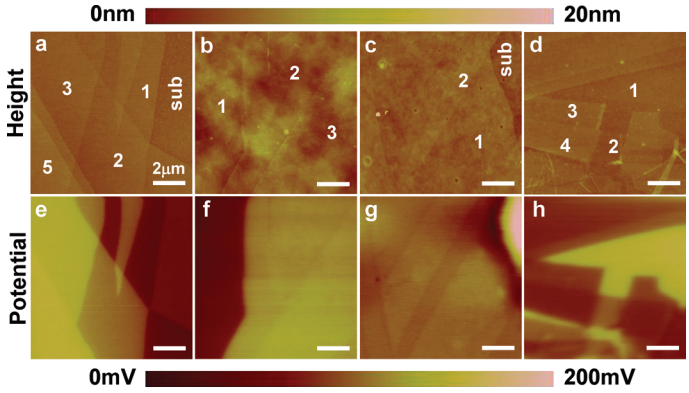


**Figure 3. Topographic and surface potential (SP) images of thin film graphene flakes deposited on various substrates. (a−d) Topography of graphene on $SiO_2$, FTS, PMMA, and ATS surfaces, respectively. The layer numbers of the graphene samples, as marked in the corresponding regions, are identified by the topographic height combined with the Raman spectra. (e−h) Simultaneously acquired SP images of the graphene samples shown in panels a−d.**

mapping showed that the potential of the same layer in a graphene sheet was relatively homogeneous (within the instrument noise level of 10 mV), indicating that the electronic properties of graphene were not significantly influenced by individual charge impurities or defects in the substrates. In contrast, there were remarkable differences in the SP between the graphene layers. Datta *et al.* has demonstrated that dipoles formed at the interface as a consequence of charge transfer between graphene and the substrate.[24] The observed potential variation between different graphene layers was likely due to the incomplete screening of dipoles with limited carrier density in graphene.[24,25] Accordingly, the different behaviors of SP on various surfaces were easily understood, as shown in Figure 3e−h. The SP of graphene on $SiO_2$ (Figure 3e) increased monotonically with the layer number, approaching a limit for graphene containing five or more layers. The lowered SP of the SLG with respect to bulk graphite indicated that the graphene on $SiO_2$ was p-doped at ambient conditions. The SLG on FTS (Figure 3f) showed a less reduced SP compared with the samples on $SiO_2$. On the other hand, the different layers of graphene flakes on the PMMA surface only exhibited little variation in SP (Figure 3g). On the ATS surface (Figure 3h), the SLG showed the highest SP, which

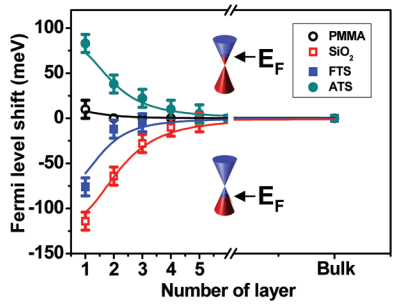


**Figure 4. The Fermi level shift of graphene on various substrates as a function of graphene thickness. The solid fitted line indicates the power law decay of the carrier concentration with increasing layer number.**

decreased with increasing graphene layers, indicative of n-type doping of graphene.

The injection of carriers from the modified substrates led to the shift of the Fermi level of graphene in the range from −130 to 90 meV, which varied as a function of graphene thickness (Figure 4). The fitted line shows a power law dependence of SP on the graphene thickness, indicating the interlayer screening length was approximately five layers.[24] We believe that the silane or polymer molecules on the substrates only determined the density and type of the carriers injected into the graphene without affecting the screening ability of graphene. Based on the Fermi energy equation

$$n(E_F) = \frac{1}{\pi}\left(\frac{E_F}{\hbar V_F}\right)^2$$

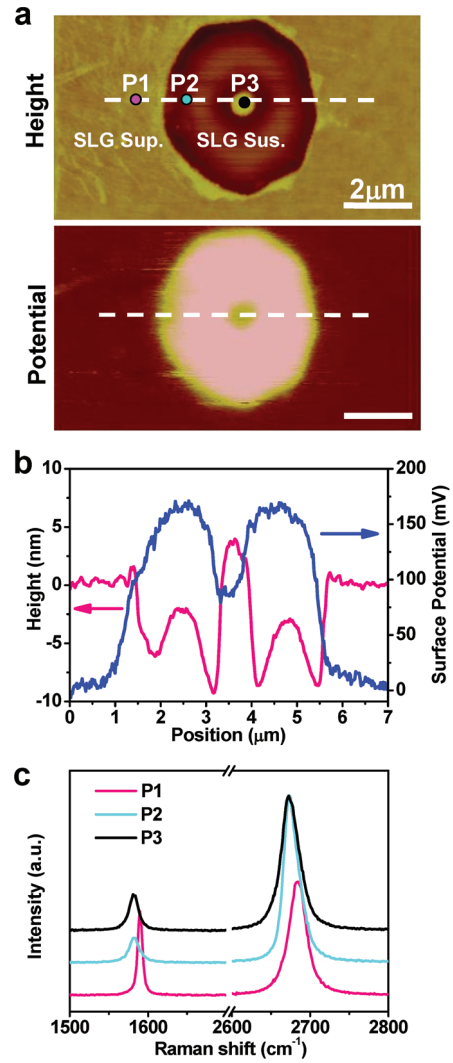


**Figure 5. A SLG sample suspended over a 5 μm diameter hole with a pillar in the center. (a) The topography and surface potential images of the SLG. (b) The cross-section analysis of the height (red) and SP (blue) of the SLG along the dash line shown in panel a. (c) The comparison of the Raman spectra between suspended and supported SLG (at position 1, 2, and 3 in panel a). (The central feature seen in the surface potential image (b) corresponds to the segment of graphene supported on the pillar.)**

where the Fermi velocity $|V_F| = 1.0 \times 10^6$ m/s and $\hbar$ is the Planck constant,[1,2] we calculated that the carrier density $n(E_F)$ of graphene on $SiO_2$ with a $-130$ meV Fermi level shift was on the order of the magnitude to $10^{12}$ cm$^{-2}$, which was equal to the application of an electric gate of $-15$ V to a graphene transistor on a 300 nm $SiO_2$ layer.[1]

Further experiments were conducted on suspended graphene membranes to elucidate the substrate effect on the carrier distribution in graphene. Figure 5a shows the topographic and SP images of a SLG sample suspended over a 5 μm diameter hole with a 0.5 μm diameter pillar in the center. The depth of the hole was around 200 nm, verifed *via* AFM measurement. It was observed that the graphene membrane adhered to the vertical wall of the hole for 5−15 nm. This was likely due to the van der Waals interactions between graphene and the $SiO_2$ sidewalls.[26,27] The cross-section analysis (Figure 5b) indicated that the SP of the suspended SLG was much higher than the SP in contact with $SiO_2$ and was close to that of bulk graphite. The difference between the suspended and supported graphene sheets became less noticeable with the increasing layer number (see Supporting Information Figure S1). In addition, the Raman spectra of the suspended SLG were similar to that of graphene on the PMMA in terms of $I$(2D)/$I$(G) and the G band frequency (Figure 5c). These observations indicated that the suspended graphene was charge neutral,[28,29] supporting the assumption that the doping of graphene originated predominantly from the effect of substrates or molecular adsorbates on the surface. For instance, the SiOH group on $SiO_2$ surface likely acted as an electron acceptors and induced a charge exchange with graphene,[30,31] which led to p-doping of graphene as well as the formation of dipoles at the interface. As graphene thickness increased, the electric field of the interface dipole was screened more efficiently, yielding less Fermi level shifts for graphene composed of five or more layers. The PMMA layer prevented graphene from being doped because of the lack of dipolar molecules or chemical groups. In contrast, silane with various functional groups has been proven to be a facile means for controlling the charge exchange and tuning, in a wide range, the Fermi level of graphene. Similar effects have been also observed in other experiments where the samples were deposited on a hydrophobic organic layer[32] or modified $SiO_2$ surface.[25]

## CONCLUSIONS

We investigated the substrate effects on the doping level of graphene by comparing the substrate-supported and freely suspended graphene samples using Raman and KFPM. The type and density of carriers injected into graphene could be well controlled by modifying the substrate with silane or polymer molecules with different functional groups. Both n- and p-doped air stable SLG samples were achieved with carrier concentrations up to $10^{12}$ cm$^{-2}$.

## METHODS

**Preparation of Various Substrates and Graphene Samples.** The graphene flakes were deposited on various substrates by mechanical exfoliation of natural graphite crystals using Scotch tape. The highly doped Si substrate with 300 nm $SiO_2$ was precleaned by oxygen plasma (FEMTO from Diener Electronic) for 2 min with a power of 40 W. Polymethyl methacrylate (PMMA, molecular mass 950 K, 4% in chlorobenzene) was spun on Si substrate at 3500 rpm for 60 s, followed by a bake out at 180 °C for 5 min. The thickness of the PMMA layer was about 270 nm. Two kinds of silanes, $(CF_3)(CF_2)_5(CH_2)_2Si(OC_2H_5)_3$ and $(NH_2)(CH_2)_3Si(OC_2H_5)_3$ (referred to as FTS and ATS, respectively), were used to modify the $SiO_2$ surfaces *via* chemical vapor deposition at room temperature.

**Raman Spectroscopy.** Raman spectra were obtained using a micro-Raman spectroscope (Renishaw inVia Raman spectroscope) at the excitation wavelength of 514 nm. The laser power was 1.0 mW to avoid a heating effect. A 100× objective lens with a NA = 0.95 was used to focus the laser beam to about 0.6 μm. The fwhm, intensity, and position of the G band and 2D band were obtained by fitting the Raman spectra with a Voigt function.

**Surface Potential Measurement with KPFM.** An atomic force microscope (AFM) (Veeco Dimension 3100) with a conductive tip was used to perform the topographic and surface potential (SP) measurements under a dual-pass tapping mode. Topography information was acquired on the first pass. During the second pass along the same scan line, the tip was lifted over the surface and applied by an oscillating voltage to generate the vibration of the probe. The amplitude of the oscillating tip was proportional to the tip−sample potential difference. The feedback controller monitored the vibrating amplitude of probe and recorded the potential difference to construct the surface potential image. We used Pt/Ir coated highly doped silicon tips (Veeco, SCM-PIT) with a nominal curvature radius of 15 nm. The tip lifted height was 10 nm. Therefore, the spatial resolution of the obtained surface potential images was estimated to be 30 nm.

*Acknowledgment.* This work was supported by the National Basic Research Program of China (No. 2007CB936802) and the Chinese Academy of Sciences (No. KJCX-YW-M04). Financial support from the National Science Foundation of China (No. 20973046) is also gratefully acknowledged.

*Supporting Information Available:* Table S1 for the water contact angle measurements on various substrates. Figure S1 for the surface potential variation between suspended and supported graphene films with different thickness. This material is available free of charge *via* the Internet at http://pubs.acs.org.

## REFERENCES AND NOTES

1. Novoselov, K. S.; Geim, A. K.; Morozov, S. V.; Jiang, D.; Zhang, Y.; Grigorieva, S. V.; Firsov, A. A. Electric Field Effect in Atomically Thin Carbon Films. *Science* **2004**, *306*, 666–669.
2. Zhang, Y.; Tan, Y.-W.; Stormer, H. L.; Kim, P. Experimental Observation of the Quantum Hall Effect and Berry's Phase in Graphene. *Nature* **2005**, *438*, 201–204.
3. Bolotin, K. I.; Sikes, K. J.; Jiang, Z.; Klima, M.; Fudenberg, G.; Hone, J.; Kim, P.; Stormer, H. L. Ultrahigh Electron Mobility in Suspended Graphene. *Solid State Commun.* **2008**, *146*, 351–355.

4. Wang, X.; Ouyang, Y.; Li, X.; Wang, H.; Guo, J.; Dai, H. Room-Temperature All-Semiconducting Sub-10nm Graphene Nanoribbon Field-Effect Transistors. *Phys. Rev. Lett.* **2008**, *100*, 206803.
5. Brant, J. C.; Leon, J.; Barbosa, T. C.; Araujo, E. N. D; Archanjo, B. S.; Plentz, F.; Alves, E. S. Hysteresis in the Resistance of a Graphene Device Induced by Charge Modulation in the Substrate. *Appl. Phys. Lett.* **2010**, *97*, 042113.
6. Sze, S. M. *Physics of Semiconductor Devices*, version 2; Wiley: New York, 2001; Chapter 5.
7. Zhang, P.; Tevaarwerk, E.; Park, B.; Savage, D. E.; Celler, G. K.; Knezevic, I.; Evans, P. G.; Eriksson, M. A.; Lagally, M. G. Electronic Transport in Nanometre-Scale Silicon-on-Insulator Membranes. *Nature* **2006**, *439*, 703–706.
8. Wang, X.; Li, X.; Zhang, L.; Yoon, Y.; Weber, P. K.; Wang, H.; Guo, J.; Dai, H. N-Doping of Graphene through Electrothermal Reactions with Ammonia. *Science* **2009**, *324*, 768–771.
9. Barraza-Lopez, S.; Vanevic, M.; Kindermann, M.; Chou, M. Y. Effects of Metallic Contacts on Electron Transport through Graphene. *Phys. Rev. Lett.* **2010**, *104*, 076807.
10. Yu, Y. J.; Zhao, Y.; Ryu, S.; Brus, L. E.; Kim, K. S.; Kim, P. Tuning the Graphene Work Function by Electric Field Effect. *Nano Lett.* **2009**, *9*, 3430–3434.
11. Lin, Y.-Y.; Gundlach, D. J.; Nelson, S. E.; Jackson, T. N. Stacked Pentacene Layer Organic Thin-Film Transistors with Improved Characteristics. *IEEE Electron Device Lett.* **1997**, *18*, 606–608.
12. Kobayashi, S.; Nishikawa, T.; Takenobu, T.; Mori, S.; Shimoda, T.; Mitani, T.; Shimotani, H.; Yoshimoto, N.; Ogawa, S.; Iwasa, Y. Control of Carrier Density by Self-Assembled Monolayers in Organic Field-Effect Transistors. *Nat. Mater.* **2004**, *3*, 317–322.
13. Campbell, I. H.; Kress, J. D.; Martin, R. L.; Smith, D. L.; Barashkov, N. N.; Ferraris, J. P. Controlling Charge Injection in Organic Electronic Devices Using Self-Assembled Monolayers. *Appl. Phys. Lett.* **1997**, *71*, 3528–3530.
14. Graf, D.; Molitor, F.; Ensslin, K.; Stampfer, C.; Jungen, A.; Hierold, C.; Wirtz, L. Spatially Resolved Raman Spectroscopy of Single- and Few-Layer Graphene. *Nano Lett.* **2007**, *7*, 238–242.
15. Ferrari, A. C.; Meyer, J. C.; Scadaci, V.; Casiraghi, C.; Lazzeri, M.; Mauri, F.; Piscanec, S.; Jiang, D.; Novoselov, K. S.; Roth, S.; *et al*. Raman Spectrum of Graphene and Graphene Layers. *Phys. Rev. Lett.* **2006**, *97*, 187401.
16. Yan, J.; Zhang, Y.; Kim, P.; Pinczuk, A. Electric Field Effect Tuning of Electron-Phonon Coupling in Graphene. *Phys. Rev. Lett.* **2007**, *98*, 166802.
17. Das, A.; Pisana, S.; Chakraborty, B.; Piscanec, S.; Saha, S. K.; Waghmare, U. V.; Novoselov, K. S.; Krishnamurthy, H. R.; Geim, A. K.; Ferrari, A. C.; *et al*. Monitoring Dopants by Raman Scattering in an Electrochemically Top-Gated Graphene Transistor. *Nat. Nanotech.* **2008**, *3*, 210–215.
18. Pisana, S.; Lazzeri, M.; Casiraghi, C.; Novoselov, K. S.; Geim, A. K.; Ferrari, A. C.; Mauri, F. Breakdown of the Adiabatic Born−Oppenheimer Approximation in Graphene. *Nat. Mater.* **2007**, *6*, 198–201.
19. Krauss, T. D.; Brus, L. E. Charge, Polarizability, and Photoionization of Single Semiconductor Nanocrystals. *Phys. Rev. Lett.* **1999**, *83*, 4840–4843.
20. Cherniavskaya, O.; Chen, L. W.; Weng, V.; Yuditsky, L.; Brus, L. E. Quantitative Noncontact Electrostatic Force Imaging of Nanocrystal Polarizability. *J. Phys. Chem. B* **2003**, *107*, 1525–1531.
21. Cui, X.; Freitag, M.; Martel, R.; Brus, L. E.; Avouris, P. Controlling Energy-Level Alignments at Carbon Nanotube/Au Contacts. *Nano Lett.* **2003**, *3*, 783–787.
22. Puntambekar, K.; Dong, J.; Haugstad, G.; Fribie, C. D. Structural and Electrostatic Complexity at a Pentacene/Insulator Interface. *Adv. Funct. Mater.* **2006**, *16*, 879–884.
23. Chen, L. W.; Ludeke, R.; Cui, X. D.; Schrott, A. G.; Kagan, C. R.; Brus, L. E. Electrostatic Field and Partial Fermi Level Pinning at the Pentacene−$SiO_2$ Interface. *J. Phys. Chem. B* **2005**, *109*, 1834–1838.
24. Datta, S.; Strachan, D. R.; Mele, E. J.; Johnson, A. T. C. Surface Potentials and Layer Charge Distributions in Few-Layer Graphene Films. *Nano Lett.* **2009**, *9*, 7–11.
25. Shi, Y.; Dong, X.; Chen, P.; Wang, J.; Li, L.-J. Effective doping of Single-Layer Graphene from Underlying $SiO_2$ Substrates. *Phys. Rev. B* **2009**, *79*, 115402.
26. Lee, Ch. G.; Wei, X. D.; Kysar, J. W.; Hone, J. Measurement of the Elastic Properties and Intrinsic Strength of Monolayer Graphene. *Science* **2008**, *321*, 385–388.
27. Bunch, J. S.; Verbridge, S. S.; Alden, J. S.; Zande, A. M. v. d.; Parpia, J. M.; Craighead, H. G.; McEuen, P. L. Impermeable Atomic Membranes from Graphene Sheets. *Nano Lett.* **2008**, *8*, 2458–2462.
28. Ni, Zh. H.; Yu, T.; Luo, Zh. Q.; Wang, Y. Y.; Liu, L.; Wong, Ch. P.; Miao, J. M.; Huang, W.; Shen, Z. X. Probing Charged Impurities in Suspended Graphene Using Raman Spectroscopy. *ACS Nano* **2009**, *3*, 569–574.
29. Berciaud, S.; Ryu, S.; Brus, L. E.; Heinz, T. F. Probing the Intrinsic Properties of Exfoliated Graphene: Raman Spectroscopy of Free-Standing Monolayers. *Nano Lett.* **2009**, *9*, 346–352.
30. Asay, D. B.; Kim, S. H. Evolution of the Adsorbed Water Layer Structure on Silicon Oxide at Room Temperature. *J. Phys. Chem. B* **2005**, *109*, 16760–16763.
31. Asay, D. B.; Barnette, A. L.; Kim, S. H. Effects of Surface Chemistry on Structure and Thermodynamics of Water Layers at Solid−Vapor Interfaces. *J. Phys. Chem. C* **2009**, *113*, 2128–2133.
32. Lafkioti, M.; Krauss, B.; Lohmann, T.; Zschieschang, U.; Klauk, H.; Klitzing, K.; Smet, J. H. Graphene on a Hydrophobic Substrate: Doping Reduction and Hysteresis Suppression under Ambient Conditions. *Nano Lett.* **2010**, *10*, 1149–1153.